A Comparison of Laser-Correction Approaches for Planar Near-Field Scanners

Scott T. McBride, Ping Yang, Robert L. Luna
MI Technologies
Suwanee, GA, USA

smcbride@mitechnologies.com, pyang@mitechnologies.com, rluna@mitechnologies.com

***Abstract*—MI has recently developed and installed two separate real-time laser-correction mechanisms for large planar scanners. One mechanism employs a spinning laser, while the other uses a tracking laser with multiple SMR constellations. The spinning-laser system is limited to planarity correction, and is appropriate for any planar scanner up to a diagonal of about 15 meters. The tracking-laser system compensates X, Y, and Z, and is intended for a horizontal planar scanner of larger size or when X and Y positions also require dynamic correction. This paper will provide an overview of the two correction mechanisms, contrast the two approaches, and include measured performance data on scanners employing each mechanism.**

I. Introduction

Conventional planar near-field (PNF) measurements require that RF samples be obtained in a plane of constant AUT Z with uniform X and Y spacing within that plane. Deviations from that plane or the regular X-Y grid lead to uncertainty in the PNF output [1]. The amount of uncertainty increases with the size of the deviations and with the test frequency.

Lasers are often used [2-5] to dynamically correct for X-Y and/or Z errors when moving a probe through a plane. This paper restricts its discussion to two specific implementations of a horizontal planar scanner, one using a tracking laser [5] and the other using a spinning laser. Both of these implementations make use of laser measurements during the acquisition combined with off-line maps created with the laser.

Figure 1 shows the MI-815-26x20 horizontal planar near-field (HPNF) scanner with the spinning-laser correction capability installed. The scan area of this system is 8m x 6m (26' by 20') and the probe is about 5.5m off the floor. The spinning laser is mounted on a separate post in the back-right corner of Figure 1. A pair of laser targets is mounted above the probe on the carriage. The carriage travels along the Y-axis rails. The 6-meter Y beam travels along the rails of the two 8-meter X beams.

Figure 2 illustrates the MI-815-66x66 HPNF scanner that uses the tracking laser. The scan area of this system is 20m x 20m (66' by 66') and the probe is approximately 21m above the floor. The laser tracker is mounted in the upper left-hand corner of the scanner in Figure 2. The probe carriage scans along the rails on the blue Y-beam. The Y beam steps along the X rails on the two green X beams.

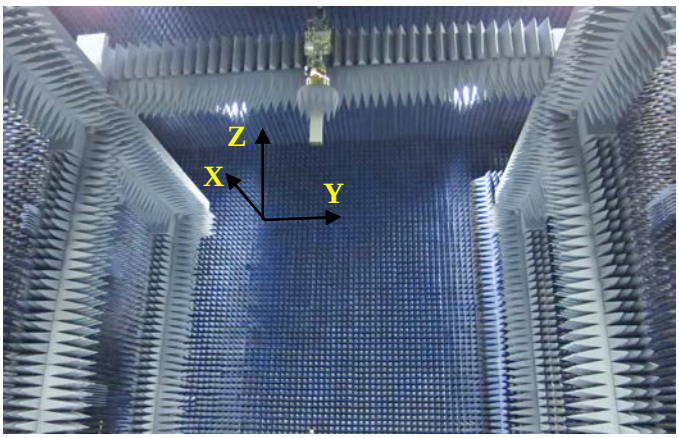

Figure 1. MI-815-26x20 8m x 6m HPNF scanner

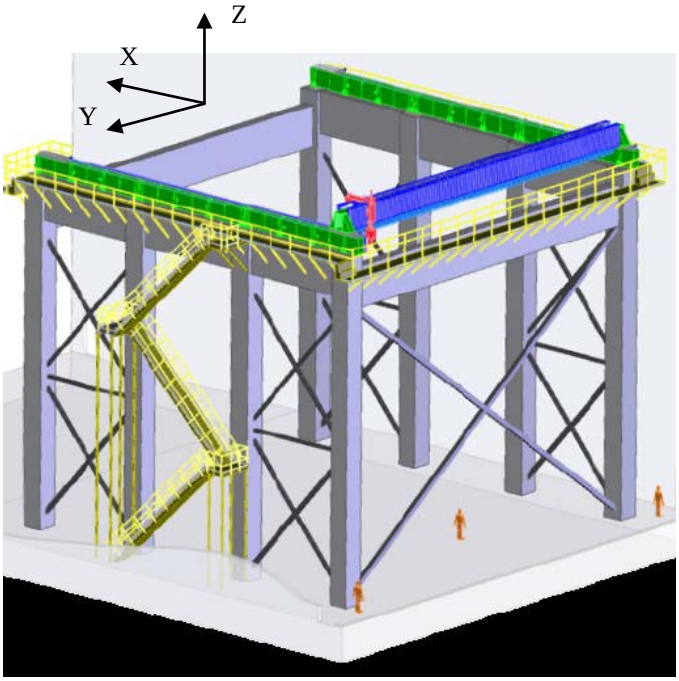

Figure 2. MI-815-66x66 20m x 20m HPNF scanner

II. System Overviews

Both systems use a combination of open-loop and closed-loop real-time correction. The closed-loop control involves laser measurements during each RF acquisition. The open-loop control involves static correction maps that are measured with the corresponding laser and loaded into the MI-710C position controller as part of an automated calibration procedure.

A. *Spinning Laser*

The spinning-laser system employs a Hamar L-740 spinning laser and a pair of Hamar A-1519 laser targets to establish and track a plane. The laser targets, which measure and report the distance from the laser beam to the targets' centers, are mounted on the probe carriage such that they are a fixed distance from the probe. (A numeric offset is measured and then applied to one of the targets allowing the two targets to be imperfectly aligned.) The MI-710C position controller has the capability to interface directly to the laser targets, using their data as one input to drive the carriage Z axis so the targets remain centered on the laser plane. Two targets are used so that no counter-steering of the targets is required and at least one target is always available.

The control loop within the MI-710C operates not only on the real-time readings from the laser targets during the acquisition, but also on X- and Y-axis positions, velocities, and accelerations in conjunction with an off-line map of $\Delta Z(X,Y)$. The configuration and tuning of the control loop can be done via the MI-710C's web-page interface, or the optional MI-3066 Single-Axis Laser-Correction Software is available to greatly streamline that process.

B. *Tracking Laser*

The tracking-laser system [5] includes a Faro Vantage laser tracker, several spherically mounted retroreflectors (SMRs), Spatial Analyzer™ software from New River Kinematics, and MI-3067 software from MI Technologies. The system automatically characterizes and then monitors the locations, attitudes, and distortions of several range features, from which it estimates the path the probe needs to follow to sample the desired X-Y grid a fixed Z distance from the AUT. A verification mode tracks and measures the probe location in range coordinates during a raster acquisition.

An inconvenient truth regarding an HPNF scanner that is 20 meters or more in each dimension is that nearly everything in the range will be changing size with even slight changes in temperature. Addressing this reality was not a trivial exercise, and led to much of the complexity in this system. As one example, mounting the laser anywhere except at the AUT location causes the laser frame to be unsuitable as the reference coordinate system for the corrections. This leads to the need for a robust range coordinate system, as well as a way to monitor the AUT location in that coordinate system.

The tracking-laser system uses as element of its approach a set of 1D maps $\Delta X(Y_i)$ and $\Delta Z(Y_i)$. These maps are produced as part of an automated calibration procedure and remain fixed until the next calibration (if any). The laser measurements made during the acquisition are used to estimate changes in location and shape since calibration of the Y beam the probe rides upon.

III. COMPARISONS

This section compares and contrasts the spinning-laser and tracking-laser approaches.

A. *Assumptions*

1) Spinning laser: This system makes the explicit assumption that the laser beam defines the proper probe Z. This implies the further assumptions that the laser sweeps a plane, and that that laser plane remains fixed with respect to the AUT throughout RF data acquisition.

This system also makes the assumption that X and Y errors are negligible or will be corrected by other means.

2) Tracking laser: The approach to this system design started with the assumption that nearly everything in the range would be changing size and shape during the course of data acquisition. A few simplifying assumptions were made:

- If Z is defined normal to the floor, then the AUT's X-Y location is assumed not to change during the acquisition.
- The floor is assumed to grow or shrink radially relative to any reference point on the floor near the center of the scan area.
- There is assumed to be no twist or rotation over time or X travel of the Y beam about the range Y axis.
- The correcting axes have reasonable orthogonality, accuracy, and straightness.
- The mechanical drift of the 3D probe-positioning errors is assumed to be limited to low spatial frequencies vs. indicated Y.

B. *Dimensions Dynamically Corrected*

The spinning-laser system only corrects planarity (Z). The tracking-laser system corrects X, Y, and Z.

C. *Coordinate-System Definition*

The coordinate system for the spinning laser is very straightforward. A laser detector is mounted on the probe carriage. When Z has moved to center the laser beam on the detector, the probe is defined to be at the proper Z. If the laser plane moves, then the coordinate system moves. No X-Y correction is possible or attempted using the spinning laser, so X and Y are defined by the indicated positions on those axes.

The coordinate system for the tracking laser is more complicated [5]. A constellation of range-monument SMRs is installed in a plane parallel to the floor. The center of that constellation is the range origin and the Z axis is defined to be normal to the monument plane. The AUT is assumed to lie along that Z axis, and dynamically change position only in the Z dimension. A separate SMR, typically attached to the AUT, is used to define the range-Z coordinate of the AUT. The Z component of correction, or planarity, is maintained relative to this AUT-height SMR. The range-X axis is initially defined to be parallel to the scanner's X-axis rails, and is subsequently determined from the known range-Phi coordinates of the range monuments.

D. *Loop-Closure Rate*

Both systems make laser measurements during RF data acquisition to close an outer loop in the real-time correction

process. The spinning-laser system is continuously making laser measurements at up to a 5 Hz rate. The tracking-laser measurements are made every N^{th} Y scan of the X-Y raster, with N a user-defined value, so the time between laser measurements is typically minutes or perhaps hours.

E. What Gets Measured During Acquisition

The spinning-laser system is measuring the carriage-mounted targets during each scan, applying that residual error along with the $\Delta Z(X,Y)$ map to try to reduce the error further. The tracking-laser system measures the 3D shape of the Y beam before a scan, communicating that shape parametrically to the virtual axis controlling carriage motion.

F. Primary Error Sources

1) Stability of laser mount: The stability of the spinning-laser mount is critical, while the tracking-laser mount is expected to move and is therefore compensated. Recall that the spinning laser's beam defines the path that the probe will take, such that if the beam wanders relative to the AUT, error will be introduced. Any tilt of the spinning laser head is especially problematic, as it can result in significant errors induced in probe Z. The tracking-laser system uses coordinate-system recall at user-selected intervals to cancel out any changes in laser position or attitude. It also makes its measurements only when all axes are stopped to avoid vibration-induced errors.

2) Refraction of the laser beam: This error affects both systems. It is due to the different speeds of light through air of different temperatures, pressures, and/or humidity. Both systems employ mechanisms to reduce the impact of this error source.

3) Laser-measurement errors: The spinning-laser measurements tend to be more accurate than the tracking-laser measurements. The primary difference is in the specified flatness of the single-axis spinning laser's plane vs. the angular measurement accuracy of the tracking laser's two-axis gimbal.

The spinning-laser targets are specified to have accuracy of ±0.0035mm (±0.00015"). The spinning laser itself is specified to have flatness (over the 90° of interest) of 0.25 arcseconds, or 0.0013mm/m. For a scanner of any appreciable size, even this tiny lack of flatness in the laser plane will likely dwarf the errors from the target.

The tracking laser's angular measurement accuracy is specified at one arcsecond (0.005mm/m), or four times the specs of the spinning laser. While the laser's distance measurement would be more accurate, the practical limitations on laser location cause some of the most important measurements to be primarily angular.

Note that these values from the laser manufacturers do not include the effects of laser-beam refraction through the air.

4) Movement of the AUT in the range coordinate system: If the AUT moves during RF data acquisition, the ideal correction mechanism will cause the probe path to follow that movement. The spinning-laser system makes no allowance for a change in distance between the AUT and the laser plane. The tracking-laser system monitors an AUT-height SMR to maintain a commanded probe-to-AUT separation.

G. Limitations

1) Scanner size: The spinning-laser targets do not function reliably (at least over a sufficient field of view) beyond about 15 meters from the laser. This limits the size of the PNF scanner for which the spinning-laser system is appropriate. The Faro Vantage used in the tracking-laser system is specified to work for a 3D scanner diagonal up to 60 meters.

2) Axes that can scan: The spinning-laser system can scan along either X or Y. The tracking-laser system can only perform its corrections when scanning along the Y axis.

3) Scanner orientation: The spinning-laser system can work with any PNF orientation. The tracking-laser system is currently limited to a horizontal PNF geometry in its determination of the range coordinate system.

H. Impact On Throughput

The spinning-laser system adds very little time to each acquisition. Once the Z axis has been moved to acquire the laser beam, the RF data acquisition is typically unaware that the laser is being used. Using the verification mode of the MI-3066 software adds about three seconds per scan.

The tracking-laser system makes its laser measurements with the positioning system stopped. It also measures each constellation multiple times to reduce refraction errors. A typical Y-beam constellation measurement takes about 90 seconds. A coordinate-system recall operation takes about the same length of time. A laser self-compensation operation also takes about 90 seconds. All three operations always occur at the beginning of each compensated acquisition. The frequency of those operations during the acquisition is user-controllable. At the mm-wave frequencies where this position compensation would be needed, a common setting would be about every two to four hours, or every 100-300 scans. The percentage increase in acquisition time is therefore not prohibitive.

I. Cost

The tracking-laser system is much more expensive than the spinning-laser system.

IV. MEASURED DATA

The data in this section were measured in the customers' facilities, exercising the entire scan area of each system. Each laser-compensation system offers a 'verification mode', in which laser measurements are captured, displayed, and stored during each scan of the acquisition. The spinning-laser system merely captures the laser-target readings being used in real time by the MI-710C, where those readings represent carriage travel relative to the laser plane. The tracking-laser system's verification mode makes measurements of an SMR mounted on the carriage in place of the probe, and reports those measurements in the range coordinate system relative to the AUT height.

A. Tracking-Laser System

For this 20m x 20m system, the Z axis has far more travel available (1 meter) than is required to maintain planarity. The tracking-laser system permits the user to specify (via an input for probe-AUT separation) the nominal Z value for an acquisition. Coarse acquisitions over the scan area were performed at nominal Z values of 0, -250, and -500 mm. Laser measurements were performed before every odd-numbered scan in the set of 21, and the X-axis increment was 950mm. Figure 3 shows the 1-σ error in each scan along Y, or the RMS after subtracting the mean error over the entire raster. In each of the three acquisitions at different Z, the zero-mean RMS error was less than 0.060 mm (0.0024").

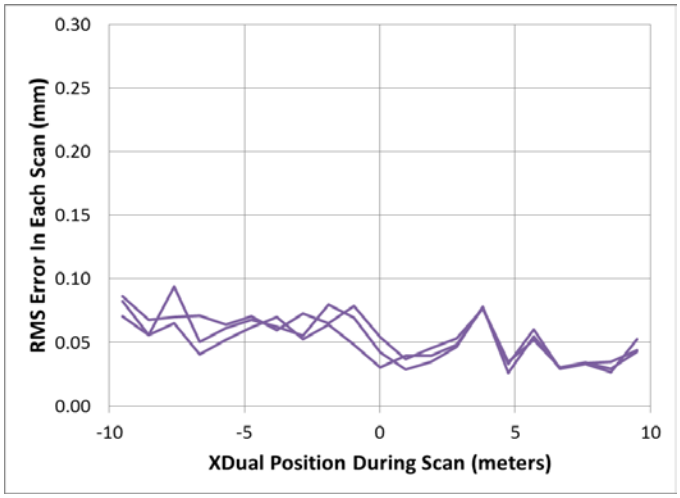

Figure 3. RMS per-scan ΔZ in three acquisitions

Figure 4 shows the 1-σ X errors measured in each scan during the same acquisitions. In each of these three acquisitions, the zero-mean RMS error (σ) was less than 0.110 mm (0.0043"). It is worth noting that the temperature had changed by about four degrees Celsius between encoder-tape installation and these acquisitions. This small temperature change caused the 20-meter X beams to expand by about a millimeter, such that 950 mm of uncorrected travel yields a mean error for that uncorrected scan of about 0.05 mm (0.002"). The laser measurements at each odd scan compensated for that error. An X-travel threshold of one meter has been recommended for this particular facility to trigger additional laser measurements in order to stay near the 0.10 mm accuracy target.

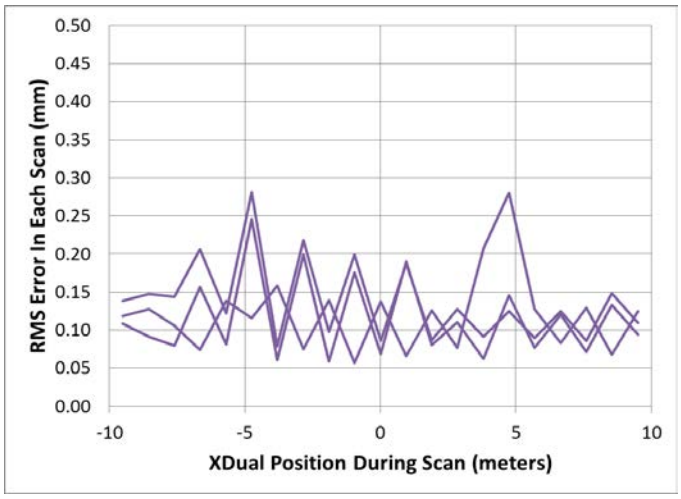

Figure 4. RMS per-scan ΔX in three acquisitions

Figure 5 shows the measured zero-mean X component of probe-carriage position error during one of the three acquisitions. Over 30,000 laser measurements are shown in Figure 5, indicating the probe's deviation from the commanded range X during each of the 21 scans. The RMS of these zero-mean errors is 0.1045 mm. The mean error removed was 0.070 mm, due primarily to the imperfect straightness and alignment of the Z axis.

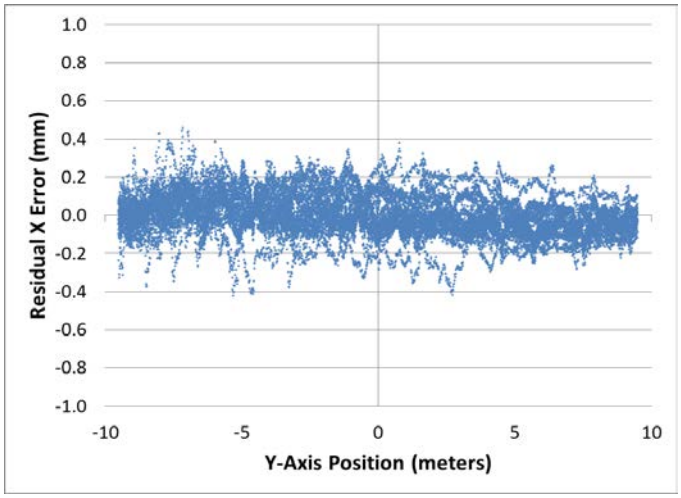

Figure 5. Tracking-laser residual X error

Figure 7 shows the zero-mean Z error during one of the three acquisitions. The RMS of the data in Figure 7 is 0.051 mm (0.002"). The removed mean of these data was 0.004 mm.

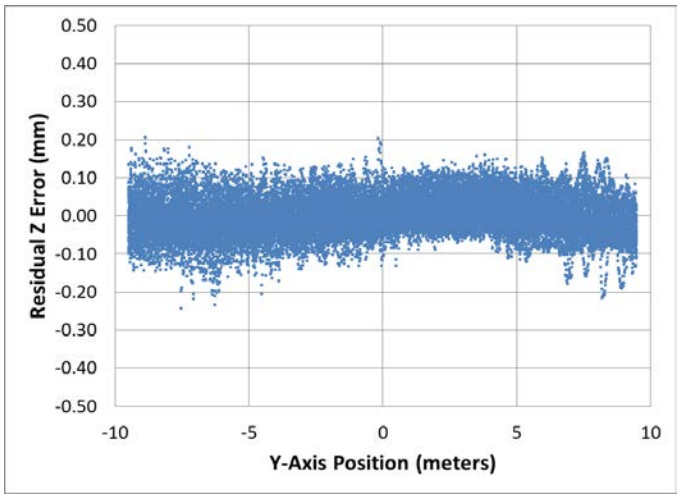

Figure 6. Tracking-laser residual Z error

The Y axis is in motion during each scan of the acquisition. In order to measure the Y errors dynamically, one would have to very tightly correlate the laser measurements with either receiver triggers or the indicated positions upon which those triggers are based. The Faro Vantage does not lend itself to such tight correlation. To quantify the compensated Y-axis accuracy, a separate series of stepped acquisitions was performed so that the laser and encoder readings need not be simultaneous. Figure 6 shows the results of those measurements, where the RMS error of each trace is no more than 0.085 mm (0.003").

Figure 7. Tracking-laser residual Y error

B. *Spinning-Laser System*

The spinning-laser system was verified over its smaller 8m x 6m scan area in two acquisitions, one scanning along Y and the other scanning along X. Figure 8 shows the results when scanning along Y at 27 different X positions. 4,000 laser measurements are shown with a mean of -0.0004 mm (-0.000016") and σ of 0.024 mm (0.001").

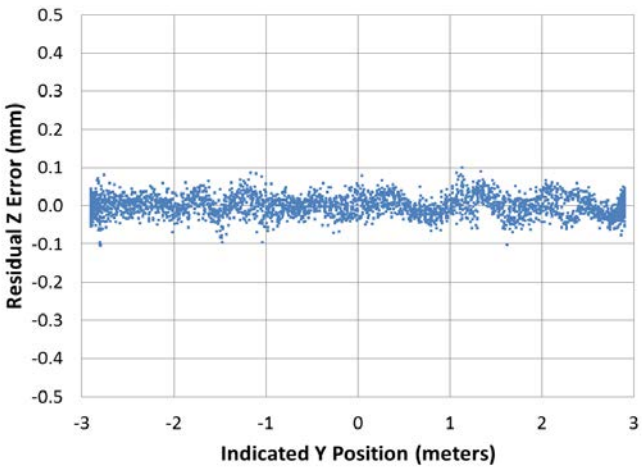

Figure 8. Spinning-laser residual for Y scans

Figure 9 represents over 6400 points taken in scans along X at 30 different Y positions. Since the entire Y beam is in motion during these scans, vibration of the probe is expected to be stronger. The mean of these measurements is -0.0003 mm (-0.000012"), and σ is 0.035 mm (0.0014").

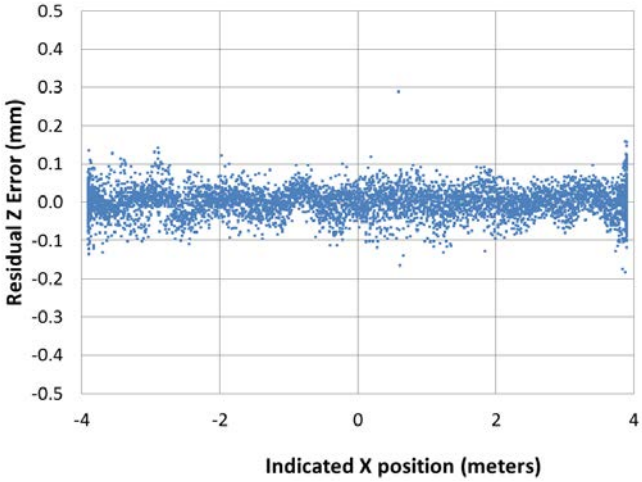

Figure 9. Spinning-laser residual for X scans

Figure 10 shows the excursion of the Z axis needed over the 8m x 6m scan area to maintain the planarity shown in Figure 8 and Figure 9. Note the 1 mm peak-to-peak range in Figure 10 compared to the residuals of σ = 0.024 and 0.035 mm.

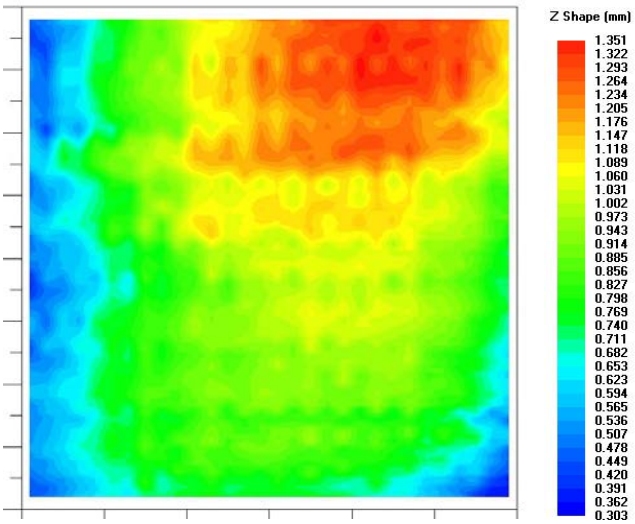

Figure 10. Planarity corrected by spinning laser

C. *Comparison of Results*

Table I. quantifies some of the key laser-correction performance measured along with relevant scanner parameters.

TABLE I. CORRECTION PERFORMANCE AND SCANNER PARAMETERS

Parameter	***Spinning laser***	***Tracking laser***
Scan Area	8m x 6m	20m x 20m
Probe height	5.5m	21m
X-Y diagonal	10m	28m
Number of laser targets	2	15
RMS planarity scanning in Y	0.024mm (0.001")	0.060mm (0.002")
RMS planarity scanning in X	0.035mm (0.0014")	N/A
RMS X-Y error	N/A	0.11mm (0.0043")

V. CONCLUSIONS

As shown in Table I., each solution provides exceptional position accuracy for scanners of these sizes. The spinning-laser system seems to be the clear choice for any PNF system where the scanner has a diagonal less than 15 meters and only planarity correction is required. The tracking-laser approach would be preferred if the scan area has a diagonal of more than 15 meters, or if dynamic position correction is also needed along X and/or Y.

ACKNOWLEDGEMENT

The authors wish to acknowledge the teams at Faro and New River Kinematics for adding several requested refinements to their products. These new capabilities were instrumental in the success of the tracking-laser approach.

The authors also wish to acknowledge Mr. Rui Shen of MI Technologies for his ideas and mechanical designs for each of the two systems.

The authors also wish to acknowledge Mr. Charles Pinson formerly of MI Technologies for his significant contributions to the spinning-laser capabilities within the MI-710C position controller.

REFERENCES

[1] A.C. Newell, "Error analysis techniques for planar near-field measurements," IEEE Trans. Antennas & Propagation, AP-36, p. 581, 1988.

[2] O.D. Asbell, J.M. Hudgens, "Field probe for the USAEPG compact range," AMTA Proceedings, pp. 9-9 to 9-12, Columbus, October, 1992.

[3] J. Way, D. Fooshe, "TRW's Astrolink near-field measurement facility," AMTA Proceedings, pp. 484-489, October, 2001.

[4] J. Way, J. Demas "A novel dual bridge near-field measurement facility," AMTA Proceedings, pp. 301-306, October, 2012.

[5] S.T. McBride, "Closed-loop real-time PNF position compensation with a tracking laser," AMTA Proceedings, pp. 320-325, October, 2014.